

1 **Allopatric plant pathogen population divergence following disease emergence**

2

3 Andreina I. Castillo ¹, Isabel Bojanini ¹, Hongyu Chen^{2,3}, Prem P. Kandel^{2,4}, Leonardo De La
4 Fuente ², and Rodrigo P.P. Almeida ¹

5 ¹ Department of Environmental Science, Policy and Management, University of California,
6 Berkeley, CA, USA.

7 ² Department of Entomology and Plant Pathology, Auburn University, Auburn, Alabama, USA.

8 ³ Current address: Department of Entomology and Plant Pathology, North Carolina State
9 University, Raleigh, North Carolina, USA.

10 ⁴ Current address: Department of Plant Pathology and Environmental Microbiology, PennState
11 University, University Park, Pennsylvania, USA.

12

13

14 Corresponding author: rodrigoalmeida@berkeley.edu

15

16 **ABSTRACT**

17 Within the landscape of globally distributed pathogens, populations differentiate via both
18 adaptive and non-adaptive forces. Individual populations are likely to show unique trends of
19 genetic diversity, host-pathogen interaction, and ecological adaptation. In plant pathogens,
20 allopatric divergence may occur particularly rapidly within simplified agricultural monoculture
21 landscapes. As such, the study of plant pathogen populations in monocultures can highlight the
22 distinct evolutionary mechanisms that lead to local genetic differentiation. *Xylella fastidiosa* is a
23 plant pathogen known to infect and damage multiple monocultures worldwide. One subspecies,
24 *Xylella fastidiosa* subsp. *fastidiosa* was first introduced to the USA ~150 years ago, where it was
25 found to infect and cause disease in grapevines (Pierce's disease of grapevines, PD). Here, we
26 studied PD-causing subsp. *fastidiosa* populations, with an emphasis on those found in the USA.
27 Our study shows that following its establishment in the USA, PD-causing strains likely split into
28 populations in the East and West Coast. This diversification has occurred via both changes in
29 gene content (gene gain/loss events) and variations in nucleotide sequence (mutation and
30 recombination). In addition, we reinforce the notion that PD-causing populations within the USA
31 acted as the source for subsequent subsp. *fastidiosa* outbreaks in Europe and Asia.

32
33 **IMPORTANCE**

34 Compared to natural environments, the reduced diversity of monoculture agricultural landscapes
35 can lead bacterial plant pathogens to quickly adapt to local biological and ecological conditions.
36 Because of this, accidental introductions of microbial pathogens into naïve regions represents a
37 significant economic and environmental threat. *Xylella fastidiosa* is a plant pathogen with an
38 expanding host and geographic range due to multiple intra- and inter-continental introductions.

39 *X. fastidiosa* subsp. *fastidiosa*, infects and causes disease in grapevines (Pierce's disease of
40 grapevines; PD). This study focused on PD-causing *X. fastidiosa* populations, particularly those
41 found in the USA but also invasions into Taiwan and Spain. The analysis shows that PD-causing
42 *X. fastidiosa* has diversified via multiple co-occurring evolutionary forces acting at an intra- and
43 inter-population level. This analysis enables a better understating of the mechanisms leading to
44 the local adaptation of *X. fastidiosa*, and how a plant pathogen diverges allopatrically after
45 multiple and sequential introduction events.

46

47

48

49

50

51

52

53

54

55

56

57

58

59

60

61

62 INTRODUCTION

63 The worldwide distribution of microbial plant pathogens is constantly shifting. Global
64 trade and movement of infected plant material enables pathogen introductions from native and
65 endemic areas to naïve regions (1, 2). Likewise, the intentional introduction of non-native plant
66 species of agronomic and ornamental value to novel environments facilitates the host range
67 expansion of endemic pathogens (3, 4). One crucial factor in the formation of novel plant-
68 pathogen associations is the amount of genetic diversity on which natural selection can act, in
69 other words, the adaptive potential (5). Differences in adaptive potential between host and
70 microbial populations can have a significant role in determining the host and geographic range of
71 a pathogen. For instance, in the case of plant pathogens, higher genetic diversity in effector
72 proteins and virulence genes has a positive effect on host range (6–9). Alternatively, multiple
73 studies have highlighted how reduced genetic diversity in plant hosts can enhance the spread of
74 pathogens within a population (10–12).

75 Factors that influence genetic diversity, whether via the action of distinct evolutionary
76 mechanisms (13, 14) or as a product of ecological and evolutionary history, affect adaptive
77 potential (15). In plant pathogens, geographical and ecological specialization have been
78 frequently described (16, 17). This is partly explained by plant pathogen differentiation and
79 specialization occurring rapidly within agricultural systems (14, 18, 19). Overall, it is expected
80 that in the absence of gene flow, plant pathogens of agricultural crops will rapidly adapt to local
81 environmental, ecological, and biological conditions (20, 21). Therefore, understanding the
82 mechanisms leading to pathogen adaptation, either to a new crop or environmental condition, has
83 great relevance in developing effective management and control strategies (22). This is
84 particularly pertinent in plant pathogens with a proven capacity to adapt to multiple crops as well

85 as having an expanding geographic and host range. This is the case of the emerging pathogen
86 *Xylella fastidiosa* (23).

87 The bacterial species *X. fastidiosa* has been reported to infect 563 plant species from 82
88 distinct botanical families (23). However, the host range of *X. fastidiosa* varies among and within
89 described subspecies and phylogenetic clades (24). The geographic distribution of the three main
90 *X. fastidiosa* subspecies is also unique, with most of them having experienced one or several
91 dispersal and establishment events at the continental scale. For this reason, efficient
92 identification and tracking of *X. fastidiosa* subspecies has important implications for the
93 development of adequate disease control and mitigation strategies (25, 26). Three *X. fastidiosa*
94 subspecies have an ancestrally allopatric range that has recently expanded: *X. fastidiosa* subsp.
95 *multiplex* is native to temperate and subtropical North America (27, 28), and has been introduced
96 multiple times into Europe (29); *X. fastidiosa* subsp. *pauca* is native to South America (28) but
97 has been recently reported in the Apulian region in Italy and in Costa Rica (30, 31); finally, *X.*
98 *fastidiosa* subsp. *fastidiosa* is native to Central America (32, 33), and was introduced to the USA
99 (24, 34), and subsequently to Europe (35) and Taiwan (36). Other non-monophyletic but
100 proposed subspecies include *X. fastidiosa* subsp. *sandyi*, found in Southern regions of the United
101 States (37, 38) and also introduced into Europe (39); and *X. fastidiosa* subsp. *morus*, only found
102 in regions where subsp. *multiplex* and subsp. *fastidiosa* co-occur (24, 40).

103 The hypothesis that subsp. *fastidiosa* was introduced once to the United States (USA)
104 ~150 years ago leading to the emergence of Pierce's Disease of grapevines (PD) is well
105 supported (24, 33, 41). PD is a grapevine malady that results in significant economic losses to
106 the wine industry in California (42) and the Southeast USA (43). Current knowledge of the
107 evolution of subsp. *fastidiosa* suggests that the ability to infect grapevines was acquired after its

108 introduction to the USA (33). Furthermore, there is evidence that local adaptation to
109 environmental factors has occurred in grape-infecting isolates across a latitudinal gradient in
110 California (34). Finally, available genomic and MLSA-E data suggest that PD-causing isolates in
111 the West and East Coast of the USA are phylogenetically distinct (34, 44)

112 These studies are indicative that after its introduction and establishment in the USA, the
113 subsp. *fastidiosa* clade causing disease in grapevines dispersed to different geographic regions
114 and diversified genetically to adapt to a range of biotic and abiotic conditions. To better
115 understand how *X. fastidiosa* evolved with the emergence of a novel plant disease (PD) and
116 diversified in allopatry in different regions of the USA, we studied populations of the pathogen
117 from the USA and abroad. We evaluated the evolutionary relationship between both USA
118 populations and their relationship with recent introduction events derived from them (i.e.
119 introductions to Spain and Taiwan associated with the emergence of PD in those regions). In
120 addition, we identified the evolutionary mechanisms facilitating population diversification by
121 defining intra-population patterns of gene gain/loss, intra-subspecific recombination, and
122 nucleotide diversity.

123

124 **RESULTS**

125 **PD isolates are split into regional clades within the USA, with Europe and Asia**
126 **introductions originating from these regions.** We arbitrarily split grapevine isolates into 3
127 phylogenetically supported clades, PD-I to -III (Fig.1). These phylogenetically supported clades
128 were also observed in the non-recombinant phylogenetic tree (Fig. S1). PD-I only included
129 isolates from the Southeast USA; PD-II and PD-III were dominated by California isolates, but at
130 the base of those clades there was one isolate from Texas (PD-II) and a sister clade from Georgia

131 (PD-III). No isolates from California grapevines clustered within the PD-I clade. From the data
132 available alone, it is not possible to infer the dispersal history of the non-California isolates in
133 PD-II and PD-III (i.e. basal sister clades or introductions to California). Isolates from Taiwan
134 were phylogenetically placed within the PD-I clade, while those from Spain were nested in the
135 PD-II clade. These represent two distinct introductions, originating from different regions in the
136 USA. Isolates from the same geographic region tended to cluster together within each major
137 clade. For instance, in the PD-I clade, most Georgia isolates from Site1 (i.e. 14B1, 14B4, 14B6,
138 16B2, 15B2, 14B3, and 16B4) and Site2 (i.e. 16M5, 16M6, 16M7, 16M8, and 16M9) clustered
139 together. Isolates from each site formed separate subclades within this group (Fig. 2). Other
140 Georgia isolates from Site1 (i.e. 14B2, 14B5, 14B7, 16B1, 16B3, 16B5, and 16B6) were more
141 closely related to those from Florida and North Carolina. In a similar manner, isolates from the
142 West Coast (i.e. California) tended to group geographically. Specifically, isolates obtained from
143 Southern California (i.e. Je81, Je104, Je112, Je110, etc.) were ancestral to those from Northern
144 California (i.e. Hopland, Stag Leap, Conn-Creek, CV17-3, Je65, Je73, etc.) in the PD-III clade.

145 A total of 141 different haplotypes named using roman numerals (I-CXIV) (Fig. 1a) were
146 found in the PD-causing core genome alignment. Haplotypes were structured by geographic
147 location and largely matched the evolutionary relationships observed in phylogenetic analyses
148 (Fig. 1b,2). Overall, haplotypes were grouped similarly to the phylogenetic analyses. Isolates
149 originating from the West and East Coast were split by 979 mutations. California had the largest
150 number of haplotypes (106) as well as haplotypes with the highest frequency: XXVIII (7), XLIV
151 (6), XXXIV (5), LVIII (4), LXVI (4), LXXIII (3), and XCIV (3). On the other hand, Southeast
152 USA haplotypes (31) were generally found in low frequency (i.e. one or two isolates). In
153 addition, Southeast isolates in PD-III formed a distinct group separated from the California group

154 by 243 mutations. Likewise, GB514 (Texas, PD-II) was closely connected to California isolates,
155 from which it differentiated by 159 mutations. Isolates originating from recent introduction
156 events (i.e. Spain and Taiwan) had unique haplotypes. Spanish associated haplotypes were linked
157 to a haplotype originating from California (PD-II) and were differentiated by 61 mutations.
158 Similarly, the Taiwan haplotypes were closely linked to the haplotype group originating from
159 Southeast USA (PD-I) and differentiated by 13 mutations.

160 **Gene gain and loss events occur following subsp. *fastidiosa* introduction events.**

161 Estimated rates of gene gain/loss were highest in branches leading to the introduction of subsp.
162 *fastidiosa* from Central America. Furthermore, a total of 35 core genes were absent in the PD-
163 causing population compared to the Costa Rican isolates, while 49 core genes were present in the
164 PD-causing population but absent in the Costa Rican isolates. In addition, gene gain/loss events
165 also occurred within the USA populations. In California (Fig. S2a) gene gain/loss rates were
166 highest in the branches leading to each cluster than within clusters, but PD-III had higher gene
167 gain/loss rates compared to PD-II. Likewise, two clades were observed within the Southeast
168 USA population (Fig. S2b). The first clade was formed by isolates 16M2, 16M3, XF51_CCPM1
169 (from Georgia, clustering with PD-III), and GB514 (from Texas, clustering with PD-II); and the
170 second by the remaining Southeast USA isolates (PD-I).

171 Some unique genes were identified through estimating gene gain/loss rates within each
172 population. We found that, when considering geographical origins of isolates alone, gene
173 presence/absence was similar in PD-II and PD-III isolates regardless of geographical origin (Fig.
174 3a). In the case of PD-I, PD-II, and PD-III isolates from Southeast USA, three genes were
175 uniquely found in PD-I and nine in PD-III (Table S3). When gene gain/loss was compared
176 between PD-II and PD-III isolates from California and PD-I, three genes coding for hypothetical

177 proteins were found in PD-II and PD-III isolates from California but absent in PD-I. In addition,
178 two genes were absent in isolates from Spain but present in PD-II and PD-III isolates from
179 California. On the other hand, two genes were found in PD-I but absent in PD-II and PD-III
180 isolates from California (Fig. 3b). In addition, five genes were absent in isolates from Taiwan,
181 which was considered as the descendant population of Southeast USA (Table 1).

182 These unique genes were annotated using eggNOG-mapper and searched in the GenBank
183 and Pfam databases, using both BLAST and interproscan5 (Table 1, Table S4). Two hypothetical
184 proteins and a gene coding for the HTH-type transcriptional regulator (*prtR*) were found for PD-I
185 (Table S3); while nine were hypothetical proteins, the protein coding genes *traC_2* (DNA
186 primase), and *higB_2* (endoribonuclease) were found for the PD-III Southeast USA isolates. Two
187 of the three genes found in PD-II and PD-III isolates from California but absent in PD-I coded
188 for hypothetical proteins and one coded for an alpha/beta fold hydrolase. For the two genes
189 absent in Spain, one of them was listed as glutamate 5-kinase, and another had a conserved
190 LacZ, Beta-galactosidase/beta-glucuronidase domain. For the two genes found in PD-I but
191 absent in PD-II and PD-III isolates from California, one was annotated as a hypothetical protein
192 and the other one as a phage head morphogenesis protein. For the five genes absent in isolates
193 from Taiwan, two were annotated as site-specific DNA-methyltransferase; another two were
194 annotated as peptidoglycan DD-metalloendopeptidase family protein and hypothetical protein,
195 respectively; the last one could be a pseudo gene with unknown function.

196 **Intra-subspecific recombination events are pervasive in both the West and East**
197 **Coast.** Intra-subspecific recombination was pervasive in both populations (Fig. 4 and Fig. S3-4).
198 The *r/m* estimate (recombination to mutation rates) for the California/Spain core genome
199 alignment was 3.29, while the same estimate for Southeast USA/Taiwan core genome alignment

200 was 5.65. In the Southeast USA (Fig. 4b), recombination events were more frequently observed
201 in isolates from the PD-II/PD-III group (recipient) than in isolates from the PD-I group (donor).
202 Within the PD-II/PD-III group, the Texas isolate GB514 (PD-II) was the most frequent
203 recombinant recipient. Donor sequences for the Texas isolate originated from both PD-I and
204 from an ‘unknown’ donor (representing genetic variability present in the population but not
205 characterized in the original sampling). A total of 188 core genes were entirely contained within
206 recombinant regions in the Southeast USA population; out of this group, 101 genes were
207 classified as hypothetical proteins. The remaining recombinant core genes belonged to a variety
208 of functions (Table S5). These functions were grouped by their COG class resulting in 12 genes
209 belonging to the ‘Cellular Processes and Signaling’ class, 5 genes associated with the
210 ‘Information Storage and Processing’ class, 41 genes from the ‘Metabolism’ class, and 7 genes
211 belonging to two or more functional classes (‘Multiple Categories’). Based on gene annotation,
212 some CDs functions are related to virulence and/or host adaptation. These include vitamin B₁₂
213 import (*btuD*), ferric uptake regulation protein (*fur*), response regulator (*gacA*), virulence protein
214 (PD_1332 in Temecula1 assembly AE009442.1, COG0346), polygalacturonase (*pglA*), export
215 protein (*secB*) and ABC transporter (*uup*).

216 Likewise, sequence exchange occurred between isolates from the PD-III and the PD-II
217 clusters in California. Recombination events were observed among isolates from the same
218 geographic regions (Fig. 4a). Specifically, recombination was frequent between sequences
219 originating from the Temecula Valley in Southern California (Fig. S3). Sequences in both groups
220 acted as donors and recipients. In addition, Northern California isolates were recipients of
221 recombinant segments from Southern California. This group was also a recipient of ‘unknown’
222 sequence fragments. A total of 180 core genes were exclusively contained within these

223 recombinant regions (Table S5). Eighty-five genes were described as hypothetical proteins. The
224 remaining genes were classified by their COG as: ‘Cellular Processes and Signaling’ (19 genes),
225 ‘Information Storage and Processing’ (6 genes), ‘Metabolism’ (38 genes), and ‘Multiple
226 Categories’ (6 genes). From these genes, those with annotated function related to host
227 adaptation/virulence include: biofilm growth-associated repressor (*bigR*), periplasmic serine
228 endoprotease (*degP*) (*htrA* in Temecula1 assembly AE009442), putative TonB-dependent
229 receptor (*phuR* in Temecula1 assembly AE009442, COG1629), virulence protein (PD_1332 in
230 Temecula1 assembly AE009442.1, COG0346), sec-independent translocase protein (*tatA-D*),
231 and PhoH-like protein (*ybeZ*).

232 Based on the used genome annotations, a total of 13 recombinant genes were shared in
233 both populations. These genes were: *glk_1* and *glk_2* (glucokinases), *glmM_2* (a
234 phosphoglucosamine mutase), *glmS_1* and *glmS_2* (glutamine--fructose-6-phosphate
235 aminotransferases [isomerizing]), *grpE* (a GrpE protein), *grxD* (a glutaredoxin 4), *gshB* (a
236 glutathione synthetase), *gtab* (a UTP--glucose-1-phosphate uridylyltransferase), *pepQ* (a Xaa-
237 Pro dipeptidase), *petA* (an Ubiquinol-cytochrome c reductase iron-sulfur subunit), *petC* (an
238 ammonia monooxygenase gamma subunit), an unnamed PKHD-type hydroxylase (COG3128),
239 and a unnamed Virulence protein (COG0346).

240 **Grapevine-infecting populations in the East and West USA are largely genetically**
241 **isolated.** Nucleotide diversity (π) varied within and among populations (Table 2). Overall,
242 nucleotide diversity was higher within the Southeast USA (947 SNPs, $\pi=1.36 \times 10^{-5}$) compared
243 to California (458 SNPs, $\pi=3.22 \times 10^{-6}$). When compared to their corresponding source
244 populations, nucleotide diversity was lower within Spain (2 SNPs, $\pi=1.38 \times 10^{-7}$) and Taiwan (6
245 SNPs, $\pi=4.15 \times 10^{-7}$). When diversity in phylogenetically distinct clusters was evaluated, PD-I

246 (93 SNPs, $\pi=7.58 \times 10^{-07}$) and PD-II (114 SNPs, $\pi=9.65 \times 10^{-07}$) had lower nucleotide diversity
247 than PD-III (509 SNPs, $\pi=3.25 \times 10^{-06}$).

248 The frequency of polymorphism present in the population in regard to expectations under
249 neutrality was calculated using a Tajima's D. Briefly, negative Tajima's D values indicate an
250 excess of rare polymorphisms than expected under neutrality, which can be caused by a selective
251 sweep or a recent population expansion. Positive Tajima's D values indicate excess of
252 intermediate frequency polymorphism than expected under neutrality, which could suggest
253 balancing selection or a recent population contraction. Tajima's D in California and the
254 Southeast USA was negative (Table 2); however, the magnitude of the statistic in California was
255 roughly twice that of the Southeast USA (-1.448 and -0.658, respectively). Due to the reduced
256 sample size, it was not possible to estimate Tajima's D in Spain or Taiwan. When populations
257 were divided phylogenetically, PD-I isolates had a lower Tajima's D (-2.060) compared to PD-II
258 (-1.781) and PD-III (-1.743). On the other hand, Watterson's θ estimates the population mutation
259 rate from the observed nucleotide diversity. This estimator decreases with increased sample size
260 or with recombination rate. Watterson's θ estimated a higher mutation rate in the Southeast USA
261 ($\theta=1.64 \times 10^{-05}$) compared to California ($\theta=5.75 \times 10^{-06}$). When populations were divided based
262 on phylogeny, mutation rate was higher in PD-III ($\theta=6.72 \times 10^{-06}$) than PD-I ($\theta=1.64 \times 10^{-06}$) or
263 PD-II ($\theta=1.87 \times 10^{-06}$).

264 In addition, F_{st} values were used to measure population differentiation across geographic
265 and phylogenetic groups. Briefly, F_{st} values compare the amount of genetic variability within
266 and between populations, values of 1 indicate complete population structuring while values of 0
267 indicate complete panmixia. Pairwise F_{st} values (Table S6) for California vs. Southeast USA
268 ($F_{st} = 0.814$) and California vs. Taiwan ($F_{st} = 0.964$) were higher than California vs. Spain (F_{st}

269 = 0.566). This was also the case for comparisons involving Southeast USA vs. Spain ($F_{st} =$
270 0.847) and Southeast USA vs. Taiwan ($F_{st} = 0.114$). Taiwan vs. Spain also showed strong
271 differentiation ($F_{st} = 0.994$). Once populations were divided phylogenetically, PD-I was more
272 differentiated from PD-II ($F_{st}=0.987$) and PD-III ($F_{st}=0.960$), than PD-II and PD-III from each
273 other ($F_{st}=0.541$).

274 An MKT was used to estimate the rate of synonymous and non-synonymous
275 polymorphism vs. the rate of synonymous and non-synonymous fixed differences across
276 geographic populations and phylogenetic groups. Under neutrality, it is expected that both rates
277 will be the same ($NI=1$). Therefore, departures of neutrality ($NI\neq 1$) will indicate either the action
278 of balancing selection (e.g. maintenance of population polymorphisms; $NI>1$) or the action of
279 positive selection (e.g. accumulation of fixed differences between populations; $NI<1$). The
280 Neutrality Index (NI) was larger than 1 in all comparisons except for Spain vs. Taiwan. NI was
281 significant only for California vs. Taiwan ($p\text{-value}=9.87\times 10e^{-05}$) (Table S6). Many
282 polymorphisms were observed in Southeast USA and California, while few were observed
283 within Spain or Taiwan. The largest number of fixed differences were observed for Taiwan vs.
284 California. When populations were divided phylogenetically, the NI values were larger than 1
285 only in comparison between PD-I with PD-II and PD-III. In this instance, the only significant NI
286 was observed for PD-I vs. PD-III ($p\text{-value}=6.26\times 10e^{-05}$). The number of polymorphisms was
287 larger in PD-III compared to PD-I and PD-II. The number of fixed differences were similar
288 between PD-I vs. PD-II and PD-III, but smaller in PD-II vs. PD-III.

289 Selective sweep signatures were pervasive in both California and Southeast USA (Fig.
290 5a), though the magnitude of the sweep was larger in California. Alternatively, CLR peaks were
291 smaller and scattered in Spain and Taiwan. When the populations were split phylogenetically,

292 CLR peaks were more numerous and prominent in PD-III, followed by PD-II, and finally PD-I
293 (Fig. 5b). Regardless if the populations were subdivided geographically or phylogenetically,
294 some CLR peaks co-located across populations, while others were group specific.

295

296 **DISCUSSION**

297 Our analyses show that after its introduction from Central America (33, 41), PD-causing
298 subsp. *fastidiosa* split into two populations: one in the East Coast (31 haplotypes) and one in the
299 West Coast (106 haplotypes). Apart from PD-II/PD-III isolates from the Southeast USA, each
300 population formed a sister monophyletic clade with long basal branch lengths. This indicates that
301 the populations split shortly after introduction to the USA. Moreover, isolates from the same
302 location clustered together, suggesting stronger sequence similarity within than between
303 locations. With the current information available, it is not possible to know if the clustering of
304 PD-II/PD-III isolates from the Southeast USA with the California clades instead of Southeast
305 USA (PD-I) reflects a recent introduction to California or if there is a higher diversity within
306 Southeast USA isolates than currently represented. Alternatively, it is feasible the East and West
307 Coast populations originated via independent introduction events. Previous studies have pointed
308 out the large genetic diversity of subsp. *fastidiosa* within Central America (33) and the
309 importation of plant material from this region into the USA (67). Our data do not exclude the
310 possibility that additional subsp. *fastidiosa* strains circulate within Central America and could
311 have been introduced to the USA in relatively simultaneous events. This is a hypothesis that
312 should be evaluated as additional whole genomic data from both native and introduced
313 populations of subsp. *fastidiosa* becomes available. However, previously published MLST data
314 (41, 67) and results based on whole genome sequence analysis (monophyly of the PD-causing

315 population, age and diversity of PD-causing clades, and their evolutionary relationship with the
316 native subsp. *fastidiosa* population) are indicative of a single introduction event.

317 Pathogen introductions into Spain and Taiwan were closely related to isolates from
318 California and the Southeast USA, respectively. Though closely related to their source
319 populations, both Spain and Taiwan had their unique core haplotypes which could be indicative
320 of early local adaptation. Nonetheless, we cannot discard the possibility that differences in
321 unique core haplotypes might also be the result of a founder effect. Small sample size in both
322 populations does not allow to test between these two possibilities; however, this should be
323 addressed once additional genomic data becomes available.

324 **Gene gain/loss events are common between and within populations.** Bacterial gene
325 content is in constant flux (68); in bacteria, evolution via gene gain and loss often precedes
326 evolution at the sequence level (i.e. nucleotide substitutions and indels) (69). Therefore
327 variations in gene content can act as a source for adaptive differentiation (70). Gene gain and
328 loss rates were highest following the introduction to the USA (e.g. 35 genes gained and 49 loss
329 vs. 4 genes gained and 5 loss between the East Coast and Taiwan); however, gene content
330 changes were also detected within each geographic population. The higher number of gene
331 gain/loss events observed in basal tree branches can be explained by a founder event. However,
332 they could also be the result of accumulated gene gain/loss events over longer evolutionary time.
333 It is likely that both factors contribute to gene gain/loss between the native and ancestral subsp.
334 *fastidiosa* populations. The highest intra-population gene gain/loss rates were localized in
335 branches following clade splits. Within California, intra-population splits were associated with
336 locations along a latitudinal gradient (PD-II in Southern California vs. PD-III in Southern and
337 Northern California). In other organisms, selection driven gene gain/loss has been described in

338 genes involved in environmental interactions (69, 71, 72). Likewise, previous studies have found
339 evidence of local adaptation to environmental conditions within California (34). Thus, it is
340 possible that changes in gene content might be adaptive to the local environment. This is further
341 supported by PD-III, which encompasses a larger latitudinal gradient, having four times higher
342 gene gain/loss rates compared to PD-II.

343 Alternatively, while gene gain/loss rates were higher in PD-II/PD-III Southeast samples
344 compared to PD-I, the difference was not as pronounced as that seen in California. Sampling of
345 PD-causing isolates has been more extensive in California; therefore, detecting environmentally
346 linked gene gain/loss might require further sampling in the Southeast USA. Based on the current
347 annotation, it is difficult to interpret the possible benefit or disadvantage of unique genes found
348 in specific *X. fastidiosa* populations. Functional analysis of these genes will be needed to
349 understand their biological role. Still, a small number of genes involved in transcription
350 regulation (*priR* and *higB_2*) and DNA replication (*traC_2*) were exclusive to PD-I and PD-III
351 Southeast USA isolates. These functions are linked to changes in bacterial transcription and
352 replication in response to environmental cues (73, 74).

353 However, it should be noted that gene gain/loss events can also be a product of non-
354 adaptive evolution. In bacteria, genetic drift promotes genome reduction and neutral gene losses
355 are favored by small population size (75, 76). In addition, homologous recombination facilitates
356 core genome homogenization but might not affect accessory genes, leading to gene content
357 divergence and pangenome expansion (69). As such, these gene gain/loss events might not be
358 linked to the adaptive potential of each population. Likewise, this could also be the case of more
359 recent introduction events and smaller population sizes (i.e. Spain and Taiwan populations).

360

361 **Unequal recombination frequencies drive inter- and intra-population**

362 **differentiation.** *r/m* estimates showed that recombination contributes more than mutation to
363 genetic diversity. The *r/m* values for California/Spain (*r/m*=3.29) and Southeast USA/Taiwan
364 (*r/m*=5.65) were higher than previous reports on subsp. *fastidiosa* (*r/m* = 2.074, (33)). However,
365 both values were lower than reports focused specifically for a California population (*r/m*=6.797,
366 (34)). Location-specific core genomes analyses can detect nucleotide changes uniquely to a
367 geographic region. Therefore, the high *r/m* found here is likely due to location-specific SNPs.

368 The number of genes located within intra-subspecific recombination was similar across
369 functional classes showing that there were no specific gene functions more prone to
370 recombination. These results are like those found in a previous analysis (33). On the other hand,
371 the frequency of recombination varied among phylogenetic clusters. PD-II/PD-III Southeast
372 isolates were recipients to sequence fragments from both PD-I and an ‘unknown’ group.
373 Similarly, recombination occurred among geographically close isolates from the PD-II and PD-
374 III clusters in California. These results show that genetic exchange is actively occurring within
375 the West and East Coast. Variations in recombination frequency across isolates have been
376 reported in native subsp. *fastidiosa* populations (33). Furthermore, recombinant genotypes form
377 distinct phylogenetic groups in subsp. *multiplex* (77). Also, *in vitro* analyses have shown that the
378 natural competency in both subsp. *fastidiosa* and subsp. *multiplex* is strain dependent (78, 79).
379 Taken together this shows that intra- and inter-subspecific recombination does not equally affect
380 all strains and that different gene functions, at least within the core genome, are not differentially
381 prone to recombination.

382 Recombination events also contribute to the differentiation between the East and West
383 Coast, as well as between PD-I, PD-II, and PD-III. Previous studies have shown allele exchange

384 between co-occurring subsp. *multiplex* and subsp. *fastidiosa* isolates in the Southeast USA, but
385 not in California (40). Therefore, the presence of multiple *X. fastidiosa* subspecies within the
386 same geographic regions can enable divergence of recombinant prone isolates or clades.
387 Moreover, highly recombinant clades also experienced higher gene gain/loss in the East and
388 West Coast. Homologous recombination can aid in maintaining core genome cohesiveness while
389 allowing extensive gene gain/loss in the accessory genome (69) and variations in gene content
390 can enable ecological divergence (80). Therefore, intra-subspecific recombination can act as a
391 source of differentiation in PD-causing isolates, not only by mediating allelic exchange but also
392 by facilitating gene gain/loss.

393 From the genes found to recombine in the Southeast USA and Californian populations
394 with putative function as host adaptation and/or virulence, most have been already identified as
395 recombinants among *X. fastidiosa* populations (79). Genes with the same annotation found in
396 both studies include *btuD*, *secB*, *uup*, *tatD*, and *ybeZ*. In other cases the identified genes were not
397 exactly the same, but genes with similar functions were found in both studies, including genes
398 related to iron acquisition (*fur* in the current study), biofilm-associated-repressor (*bigR* in the
399 current study) (81–83) and sulfide sensor (84), other members of the *sec* pathway (*tatA-D*) (85,
400 86), and other serine proteases (*degP* here) (79, 85, 86). Interestingly the vitamin B₁₂ transporter
401 BtuD was the single annotated gene with highest recombination inter- and intra-subspecific
402 identified in a previous study (79), and has been described in other bacteria as regulating gene
403 expression, abundance of microorganisms and virulence (87, 88), although no functionality has
404 been attributed yet to *X. fastidiosa*. Genes like *fur* and *gacA* have been identified as
405 transcriptionally regulated by calcium (89), an abundant element inside xylem vessels. Other
406 genes like the putative TonB-dependent receptor (*phuR* in the Temecula1 assembly AE009442,

407 COG1629), are involved in twitching motility and biofilm formation (90); and PhoH-like protein
408 (*ybeZ*), is putatively linked to detection and response to changes of phosphate concentration (91).

409 **West and East Coast populations show unique trends of genetic diversity and**
410 **mutation rate.** At a first glance, isolates originating from the Southeast USA population were
411 more genetically diverse than those originating from California. However, this trend was less
412 clear when populations were assigned phylogenetically. PD-II (California + 1 Texas isolate) had
413 slightly higher than PD-I (exclusively Southeast USA), and PD-III (California + 3 Georgia
414 isolates) had higher genetic diversity than either PD-I or PD-II.

415 The negative Tajima's D values indicate an excess of rare polymorphisms, which can be
416 caused by a selective sweep or a recent population expansion. In the case of subsp. *fastidiosa*, a
417 population expansion could have occurred following a founder effect. This result, in addition to
418 previously published data (24, 33, 67), supports the hypothesis that subsp. *fastidiosa* was
419 introduced to the USA. Furthermore, they show that limitation on genetic diversity caused by a
420 founder effect can be long lasting. Tajima's D values were markedly reduced in PD-I compared
421 to the geographic Southeast USA population (PD-I+PD-II(Texas)/PD-III(Georgia)). This is
422 indicative that there is more than one phylogenetic cluster circulating in the East Coast.
423 Similarly, Tajima's D was smaller in PD-II and PD-III compared to California, further
424 supporting the idea of ongoing latitudinal distinction within the West Coast.

425 Watterson's θ estimates were also affected by grouping criteria. In the case of Southeast
426 USA compared to PD-I, the Watterson estimator remained roughly unchanged suggesting that
427 mutation rate in the region is captured by current sampling. Watterson's θ was larger in
428 California compared to either PD-II or PD-III, and lower in PD-III compared to PD-II. The
429 values were comparable to previous reports in California (34). This could be indicative that

430 mutation rate within the West Coast is, to a certain point, location dependent and that mutation
431 itself contributes less to population differentiation than other evolutionary forces.

432 **PD-causing strains have differentiated phylogenetically and geographically.** The F_{st}
433 values for different groups of PD-causing isolates were higher than those reported for other
434 global bacterial pathogens(92). It is possible that these values reflect rapid differentiation of PD-
435 causing populations. Pairwise F_{st} values between PD-I (Southeast only) vs. PD-II (California + 1
436 Texas) and PD-III (California + 3 Georgia) were higher than between Southeast USA and
437 California. These results further support the phylogenetic and geographic separation of the East
438 and West Coast, and the more recent differentiation within California. How much this
439 differentiation can be linked to the Southeast USA PD-II/PD-III group, needs to be further
440 analyzed. Our F_{st} analyses indicate a complex phylogeographic history between USA
441 populations, yet, the effects of sample size in these calculations should not be ignored. For
442 example, recently introduced populations (e.g. Spain and Taiwan) showed even higher
443 population differentiation than comparisons involving their source populations. Whether this
444 suggests higher differentiation as a product of a founder effect remains to be determined.

445 In general, genetic diversity has a high impact on adaptive potential (93); however, some
446 genetic variants might be considered neutral and can be estimated based on the number of
447 synonymous polymorphisms (94). Variables associated with local adaptation are linked to non-
448 synonymous polymorphisms. There were more non-synonymous than synonymous
449 polymorphism in both the East and West Coast. This suggests that, though the number of
450 polymorphisms might be limited due to a recent introduction event, each population maintains a
451 certain level of genetic variation (as evidenced by $NI > 1$) which could be a source for local
452 adaptation (95).

453 When populations were divided according to their phylogenetic relationships, a
454 significant $NI > 1$ was only observed between PD-I and PD-III. Polymorphism largely
455 accumulated in PD-III compared to PD-I. However, the number of fixed differences was
456 comparable between PD-I vs. PD-II and PD-III. This shows that a significant number of intra-
457 clade polymorphisms in PD-III have not yet been fixed. Instead, fixed differences seem to mostly
458 reside between the PD-I compared to PD-II and PD-III. This further supports the idea that East
459 and West Coast populations split early following introduction to the USA, with local population
460 differentiation within a latitudinal gradient in the West Coast.

461 **Selective sweeps have occurred following the introduction of *X. fastidiosa* to the**
462 **USA.** Many CLR peaks were co-localized in the same region while others were group exclusive.
463 The localized nature of CLR peaks in the core genome alignment suggests that selective sweeps
464 can only be detected on certain genes. The location and intensity of selective sweeps are the
465 product of evolutionary and ecological variables. A founder effect can result in reduced selection
466 strength, but it might not affect recombination potential, particularly in *X. fastidiosa* (96).
467 Therefore, the CLR patterns observed here likely reflect genes undergoing strong selection,
468 either following subsp. *fastidiosa* introduction from Central America (co-localized CLR peaks)
469 or via selective pressures associated to a specific environment (group specific CLR peaks).
470 Strong CLR signals in both PD-II and PD-III are indicative that selective sweeps have been more
471 prevalent within the West Coast. Some genes located in CLR peak include: outer membrane
472 protein assembly factors (*BamA-B*), a beta-barrel assembly-enhancing protease (*bepA_4*), a
473 ubiquinol cytochrome C oxidoreductase (*fbcH*), a glycine cleavage system transcriptional
474 repressor (*gcvR*), a glutamine--fructose-6-phosphate aminotransferase (*glmS_2*), a
475 proton/glutamate-aspartate symporter (*glpP*), and a sensor histidine kinase (*rcsC*). Branch-site

476 analyzes aimed to detect signals of positive selection should be performed to further evaluate
477 these results.

478

479 CONCLUSIONS

480 We identified a series of evolutionary mechanisms that led to the diversification of PD-causing
481 subsp. *fastidiosa* populations. Diversification has occurred in core genome sequences via
482 mutation and recombination, and in gene content via gain/loss events. These differences have the
483 potential of facilitating local adaptation to environmental conditions, and in the absence of gene
484 flow, lead to pathogen specialization. The host range and geographic distribution of *X. fastidiosa*
485 is expanding and each new introduction can result in significant economic and ecological
486 damage. Understanding the mechanisms and speed of local adaptation in *X. fastidiosa* is
487 important to manage emerging *X. fastidiosa* diseases and hopefully limit the number of novel
488 epidemics.

489

490 MATERIALS AND METHODS

491 **Sampling, culturing, and isolation.** The following study encompasses 175 *X. fastidiosa*
492 subsp. *fastidiosa* isolates obtained from infected PD-symptomatic grapevines from diverse
493 geographic regions. The number of isolates from each region were: California (N=140),
494 Southeast USA (N=31), Spain (N=2), and Taiwan (N=2). In addition, three non-grapevine-
495 infecting *X. fastidiosa* subsp. *fastidiosa* isolates from Costa Rica were used as an outgroup (33).
496 New subsp. *fastidiosa* isolates were obtained from infected grapevines in the Southeast USA
497 during 2014-2016; these isolates were cultured from symptomatic leaves as previously described
498 (44). Colonies growing after ~1-2 weeks under 28°C incubation were re-streaked, cloned, and

499 had identity confirmed with *X. fastidiosa* specific PCR primer sets (45). Isolates were obtained
500 from different grapevine varieties. Specifically, the varieties found in Site1 were: Merlot (N=5,
501 years 2014-2016), Mourvedre (N=1, year 2014), Cabernet Sauvignon (N=1, year 2014),
502 Chardonnay (N=5, years 2014-2016), Viognier (N=2, years 2014-2015), Sangiovese (N=1, year
503 2014), and Touriga (N=1, year 2014). The varieties found in Site2 were: Montaluce (N=1, year
504 2015), Merlot (N=3, year 2016), Pinot grigio (N=3, year 2016), and Vidal (N=3, year 2016).
505 Except for Site1 (N=16) and Site2 (N=8), all data included in the following study has been
506 previously made publicly available. Detailed metadata on each assembly has been compiled in
507 Table S1; assembly statistics for new whole genome sequences are provided in Table S2.

508 **Sequencing, assembly, and annotation of *X. fastidiosa* subsp. *fastidiosa* isolates.** All
509 isolates were sequenced using Illumina HiSeq2000. Samples were sequenced at the University of
510 California, Berkeley Vincent J. Coates Genomics Sequencing Laboratory (California Institute for
511 Quantitative Biosciences; QB3), and the Center for Genomic Sciences, Allegheny Singer
512 Research Institute, Pittsburgh, PA. All raw reads and information regarding each newly
513 sequenced strain can be accessed under the NCBI BioProject accession PRJNA655351. The
514 quality of raw paired FASTQ reads was evaluated using FastQC (46) and visualized using
515 MultiQC (47). Low quality reads and adapter sequences were removed from all paired raw reads
516 using seqtk v1.2 (<https://github.com/lh3/seqtk>) and cutadapt v1.14 (48) with default parameters.
517 After pre-processing, isolates were assembled *de novo* with SPAdes v3.13 (49, 50) using the -
518 *careful* parameter and -k of 21, 33, 55, and 77. Assembled contigs were reordered using Mauve's
519 contig mover function (51) with the complete publicly available Temecula1 assembly
520 (GCA_000007245.1) used as reference. Assembled and reordered genomes were then

521 individually annotated using the Prokka pipeline (52). In addition, published genome sequences
522 were also re-annotated with Prokka.

523 **Core genome alignments, construction of Maximum Likelihood trees, and haplotype**
524 **network.** Roary v3.11.2 (53) was used to calculate the number of genes in the core (genes shared
525 between 99-100% strains), soft-core (genes shared between 95-99% strains), shell (genes shared
526 between 15-95% strains), and cloud (genes shared between 0-15% strains) genomes of PD-
527 causing isolates (N=175). A core genome alignment of PD-causing isolates plus the three Costa
528 Rica isolates (non-PD) was created using the -e (codon aware multisequence alignment of core
529 genes) and -n (fast nucleotide alignment) flags in Roary. This core genome alignment was used
530 to build a Maximum Likelihood (ML) tree with RAxML (54). The GTRCAT substitution model
531 was used on tree construction, while tree topology and branch support were assessed with 1000
532 bootstrap replicates. In addition, a non-recombinant tree was constructed by removing detected
533 recombinant segments from the core genome alignment (see later methods). The ML non-
534 recombinant tree was constructed using the same parameters as the recombinant tree. Finally, a
535 haplotype network for PD-causing isolates was built following removal of the outgroup
536 sequences (non-PD). Core genome haplotypes were calculated based on the number of mutations
537 among the analyzed strains, and the haplotype network was built using the HaploNet function in
538 the R package 'pegas' (55). Haplotypes were then color-coded by geographic location.

539 **Estimation of recombinant segments and gene gain/loss rates within populations.**
540 Isolates were divided based on their geographical origin: California, Southeast USA, Spain, and
541 Taiwan. California and the Southeast USA were the source population for Spain and Taiwan,
542 respectively. Source and descendant relationships between populations were phylogenetically
543 determined (see results). A core genome alignment was created for California/Spain (N=142),

544 and Southeast USA/Taiwan (N=33). The alignment was used to estimate the frequency and
545 location of recombinant events. FastGEAR (56) was used with default parameters to identify
546 lineage-specific recombinant segments (ancestral) and strain-specific recombinant segments
547 (recent). The size and location of recombinant segments across the length of the core genome
548 alignment were mapped within California/Spain and Southeast USA/Taiwan using the R package
549 ‘circlize’ (57). Donor/recipient recombinant regions were visualized using fastGEAR’s
550 plotRecombinations script. In addition, the number of substitutions introduced by recombination
551 vs. random point mutation (r/m) (58) was estimated for the California/Spain and Southeast
552 USA/Taiwan core genome alignments using ClonalFrameML (59). It should be noted that
553 fastGEAR was designed to test recombination in individual gene alignments instead of core
554 genome alignments; a previous study found that fastGEAR was more conservative than other
555 more appropriate recombination detection methods such as ClonalFrameML (34). Future
556 research should perform an empirical comparison of recombination detection methods for *X.*
557 *fastidiosa*.

558 Additionally, the stochastic probability of gene gain/loss per tree branch was estimated
559 with GLOOME using default parameters (60). Briefly, RAxML was used to build a ML
560 phylogenetic tree for the California/Spain and Southeast USA/Taiwan core genome alignments.
561 The parameters used were the same that for the PD-causing ML tree. Roary v3.11.2 was used to
562 calculate a binary gene presence (1)/absence (0) matrix within the California/Spain and the
563 Southeast USA/Taiwan populations. A binary accessory genome matrix was created by
564 removing core genome genes from the dataset. Subsequently, the binary accessory
565 presence/absence matrix was transposed and converted into FASTA format. The binary
566 accessory genome and the ML trees were used as inputs to the GLOOME analysis. Unique genes

567 were identified through estimating gene gain/loss rates within each population. These genes were
568 annotated by eggNOG-mapper v1.0.3 (<https://github.com/eggnogetdb/eggnoget-mapper>) and
569 searched in the Genebank and Pfam databases using BLAST and interproscan v5.47
570 (<https://github.com/ebi-pf-team/interproscan>).

571 **Population genomics analyses.** Global measures of genetic diversity, population
572 differentiation, and selective sweeps were estimated for the PD-causing dataset using the R
573 package ‘PopGenome’ (61). The dataset was subdivided in two ways: a) based on isolates’
574 geographical origin (i.e. California, Southeast USA, Spain, and Taiwan), and b) based on
575 isolates’ phylogenetic relationships (i.e. PD-I, PD-II, and PD-III; see results). All calculations
576 described below were performed for both the (a) geographic and (b) phylogenetic subdivisions.

577 Genetic diversity was estimated by computing nucleotide diversity (π), Tajima’s D (62),
578 and the Watterson’s estimator (θ) (63). Briefly, nucleotide diversity (π) measures the average
579 number of nucleotide differences per site in pairwise comparisons among DNA sequences.
580 Tajima’s D evaluates the frequency of polymorphism present in a population and compares that
581 value to the expectation under neutrality. The Watterson θ estimator measures the mutation rate
582 of a population. Population differentiation was estimated by calculating the Fixation Index (F_{st})
583 (64) within (a) geographic and (b) phylogenetic groups. In addition, the McDonald-Kreitman
584 Test (MKT) (65) was used to estimate the rate of synonymous (syn-P) and non-synonymous
585 (nonsyn-P) polymorphism, against the rate of fixed synonymous (syn-F) and non-synonymous
586 (nonsyn-F) differences. In each instance, the Neutrality Index (NI) was calculated. $NI > 1$
587 suggests an excess of preserved polymorphism maintained via balancing selection. Alternatively,
588 $NI < 1$ suggests population divergence via positive selection. Finally, the location and magnitude
589 of selective sweeps was calculated using Nielsen’s composite-likelihood-ratio (CLR) (66). This

590 test identifies regions with aberrant allele frequency spectra and estimates if the aberrant allele
591 distribution fits the expectations of a selective sweep. The test was performed on a 1500bp
592 sliding window across the length of the PD-causing core genome alignment.

593 **Data Availability.** The raw sequence data files for the newly published isolates were
594 submitted to the NCBI Sequence Read Archive under accession number SAMN15732826
595 through SAMN15732849. All other used data has been previously published. All accession
596 numbers are listed in Table S1.

597

598

599 **ACKNOWLEDGMENTS**

600 This work has received funding from the PD/GWSS Research Program, California Department
601 of Food and Agriculture, and the European Union’s Horizon 2020 research and innovation
602 program under grant agreement N. 727987 “*Xylella fastidiosa* Active Containment Through a
603 multidisciplinary-Oriented Research Strategy XF-ACTORS. Genome sequencing was performed
604 at the UC Berkeley Vincent J. Coates Genomics Sequencing Laboratory, which is supported by
605 an NIH instrumentation grant (S10 OD018174).

606

607 **References**

- 608 1. Pimentel D, Lach L, Zuniga R, Mprison D. 2000. Environmental and Economic Costs of
609 Nonindigenous Species in the United States. *Bioscience* 50:53.
- 610 2. Fletcher J, Bender C, Budowle B, Cobb WT, Gold SE, Ishimaru CA, Luster D, Melcher
611 U, Murch R, Scherm H, Seem RC, Sherwood JL, Sobral BW, Tolin SA. 2006. Plant
612 Pathogen Forensics: Capabilities, Needs, and Recommendations. *Microbiol Mol Biol Rev*
613 70:450–471.
- 614 3. Pyšek P, Jarošík V, Pergl J. 2011. Alien plants introduced by different pathways differ in
615 invasion success: Unintentional introductions as a threat to natural areas. *PLoS One* 6.
- 616 4. Early R, Bradley BA, Dukes JS, Lawler JJ, Olden JD, Blumenthal DM, Gonzalez P,
617 Grosholz ED, Ibañez I, Miller LP, Sorte CJB, Tatem AJ. 2016. Global threats from
618 invasive alien species in the twenty-first century and national response capacities. *Nat*
619 *Commun* 7.
- 620 5. Mable BK. 2019. Conservation of adaptive potential and functional diversity: integrating
621 old and new approaches. *Conserv Genet* 20:89–100.
- 622 6. Baltrus DA, Nishimura MT, Dougherty KM, Biswas S, Mukhtar MS, Vicente J, Holub
623 EB, Dangl JL. 2012. The molecular basis of host specialization in bean pathovars of
624 *Pseudomonas syringae*. *Mol Plant-Microbe Interact* 25:877–888.
- 625 7. Karasov TL, Horton MW, Bergelson J. 2014. Genomic variability as a driver of plant–
626 pathogen coevolution? *Curr Opin Plant Biol* 18:24–30.
- 627 8. Plissonneau C, Benevenuto J, Mohd-Assaad N, Fouché S, Hartmann FE, Croll D. 2017.
628 Using population and comparative genomics to understand the genetic basis of effector-
629 driven fungal pathogen evolution. *Front Plant Sci* 8:1–15.
- 630 9. Mokryakov M V., Abdeev IA, Piruzyan ES, Schaad NW, Ignatov AN. 2010. Diversity of
631 effector genes in plant pathogenic bacteria of genus *Xanthomonas*. *Microbiology* 79:58–
632 65.
- 633 10. Rowntree JK, Cameron DD, Preziosi RF. 2011. Genetic variation changes the interactions
634 between the parasitic plant-ecosystem engineer *Rhinanthus* and its hosts. *Philos Trans R*
635 *Soc B Biol Sci* 366:1380–1388.
- 636 11. González R, Butković A, Elena SF. 2019. Role of host genetic diversity for susceptibility-
637 to-infection in the evolution of virulence of a plant virus. *Virus Evol* 5:1–12.
- 638 12. Zhu Y, Chen H, Fan J, Wang Y, Li Y, Chen J, Fan JX, Yang S, Hu L, Leung H, Mew TW,
639 Teng PS, Wang Z, Mundt CC. 2000. Genetic diversity and disease control in rice. *Nature*
640 406:718–722.
- 641 13. Escribe F. 2012. Diversity of Plant Virus Populations: A Valuable Tool Diversity of Plant
642 Virus Populations: A Valuable Tool for Epidemiological Studies, p. 13. *In* IntechOpen.
- 643 14. Brown JKM. 2015. Durable Resistance of Crops to Disease: A Darwinian Perspective.
644 *Annu Rev Phytopathol* 53:513–539.
- 645 15. Zhan J. 2016. Population Genetics of Plant Pathogens. eLS 1–7.
- 646 16. Giraud T, Gladieux P, Gavrillets S. 2010. Linking emergence of fungal plant diseases and
647 ecological speciation. *Trends Ecol Evol* 25:387–395.
- 648 17. Mhedbi-Hajri N, Hajri A, Boureau T, Darrasse A, Durand K, Brin C, Saux MF Le,
649 Manceau C, Poussier S, Pruvost O, Lemaire C, Jacques MA. 2013. Evolutionary History
650 of the Plant Pathogenic Bacterium *Xanthomonas axonopodis*. *PLoS One* 8.
- 651 18. Zhan A, Hu J, Hu X, Zhou Z, Hui M, Wang S, Peng W, Wang M, Bao Z. 2009. Fine-scale

- 652 population genetic structure of zhikong scallop (*Chlamys farreri*): Do local marine currents
653 drive geographical differentiation? *Mar Biotechnol* 11:223–235.
- 654 19. McDonald BA, Linde C. 2002. The population genetics of plant pathogens and breeding
655 strategies for durable resistance. *Euphytica* 124:163–180.
- 656 20. Slatkin M. 1985. Gene flow in natural populations. *Annu Rev Ecol Syst* Vol 16 393–430.
- 657 21. McDermott JM, McDonald BA. 1993. Gene flow in plant pathosystems. *Annu Rev*
658 *Phytopathol* 31:353–373.
- 659 22. Pruvost O, Boyer K, Ravigné V, Richard D, Vernière C. 2019. Deciphering how plant
660 pathogenic bacteria disperse and meet: Molecular epidemiology of *Xanthomonas citri*
661 pv. *citri* at microgeographic scales in a tropical area of Asiatic citrus canker endemicity.
662 *Evol Appl* 12:1523–1538.
- 663 23. EFSA. 2018. Update of the *Xylella* spp. host plant database. *EFSA J* 16:1–87.
- 664 24. Vanhove M, Retchless AC, Sicard A, Rieux A, Coletta-filho HD, Fuente LD La, Stenger
665 DC, Almeida PP. 2019. Genomic Diversity and Recombination among *Xylella fastidiosa*
666 Subspecies. *Appl Environ Microbiol* 85:1–17.
- 667 25. Bragard C, Dehnen-Schmutz K, Di Serio F, Gonthier P, Jacques MA, Jaques Miret JA,
668 Justesen AF, MacLeod A, Magnusson CS, Milonas P, Navas-Cortés JA, Potting R,
669 Reignault PL, Thulke HH, Van der Werf W, Vicent Civera A, Yuen J, Zappalà L,
670 Makowski D, Delbianco A, Maiorano A, Muñoz Guajardo I, Stancanelli G, Guzzo M,
671 Parnell S. 2019. Effectiveness of in planta control measures for *Xylella fastidiosa*. *EFSA J*
672 17.
- 673 26. Almeida RPP, De La Fuente L, Koebnik R, Lopes JRS, Parnell S, Scherm H. 2019.
674 Addressing the New Global Threat of *Xylella fastidiosa*. *Phytopathology* 109:172–174.
- 675 27. Nunney L, Hopkins DL, Morano LD, Russell SE, Stouthamer R. 2014. Intersubspecific
676 Recombination in *Xylella fastidiosa* Strains Native to the United States: Infection of Novel
677 Hosts Associated with an Unsuccessful Invasion. *Appl Environ Microbiol* 80:1159–1169.
- 678 28. Nunney L, Yuan X, Bromley RE, Stouthamer R. 2012. Detecting Genetic Introgression:
679 High Levels of Intersubspecific Recombination Found in *Xylella fastidiosa* in Brazil. *Appl*
680 *Environ Microbiol* 78:4702–4714.
- 681 29. Landa BB, Castillo AI, Giampetruzzi A, Kahn A, Román-Écija M, Velasco-Amo MP,
682 Navas-Cortés JA, Marco-Noales E, Barbé S, Moralejo E, Coletta-Filho HD, Saldarelli P,
683 Saponari M, Almeida RPP. 2020. Emergence of a plant pathogen in Europe associated
684 with multiple intercontinental introductions. *Appl Environ Microbiol* 86:1–15.
- 685 30. Giampetruzzi A, Saponari M, Loconsole G, Boscia D, Savino VN, Almeida RPP, Zicca S,
686 Landa BB, Chacón-Díaz C, Saldarelli P. 2017. Genome-Wide Analysis Provides Evidence
687 on the Genetic Relatedness of the Emergent *Xylella fastidiosa* Genotype in Italy to
688 Isolates from Central America. *Phytopathology* 107:816–827.
- 689 31. Saponari M, Giampetruzzi A, Loconsole G, Boscia D, Saldarelli P. 2018. *Xylella*
690 *fastidiosa* in Olive in Apulia: Where We Stand. *Phytopathology* 109:175–186.
- 691 32. Nunney L, Azad H, Stouthamer R. 2019. An Experimental Test of the Host-Plant Range
692 of Nonrecombinant Strains of North American *Xylella fastidiosa* subsp. *multiplex*.
693 *Phytopathology* 109:294–300.
- 694 33. Castillo AI, Chacón-díaz C, Rodríguez-murillo N, Coletta- HD, Almeida RPP, Rica C.
695 2020. Impacts of local population history and ecology on the evolution of a globally
696 dispersed pathogen . *BMC Genomics* 21:1–51.
- 697 34. Vanhove M, Sicard A, Ezennia J, Leviten N, Almeida RPP. 2020. Population structure

- 698 and adaptation of a bacterial pathogen in California grapevines. *Env Microbiol.*
- 699 35. Gomila M, Moralejo E, Busquets A, Segui G, Olmo D, Nieto A, Juan A, Lalucat J. 2018.
- 700 Draft Genome Resources of Two Strains of *Xylella fastidiosa* XYL1732/17 and
- 701 XYL2055/17 Isolated from Mallorca Vineyards. *Phytopathology* 109:222–224.
- 702 36. Castillo AI, Tuan S-J, Retchless AC, Hu F-T, Chang H-Y, Almeidaa RPP. 2019. Draft
- 703 Whole-Genome Sequences of *Xylella fastidiosa* subsp. *fastidiosa* Strains TPD3 and TPD4,
- 704 Isolated from Grapevines in Hou-li, Taiwan. *Microbiology* 8:1–3.
- 705 37. Schuenzel EL, Scally M, Stouthamer R, Nunney L. 2005. A Multigene Phylogenetic
- 706 Study of Clonal Diversity and Divergence in North American Strains of the Plant
- 707 Pathogen *Xylella fastidiosa*. *Appl Environ Microbiol* 71:3832–3839.
- 708 38. Yuan X, Morano L, Bromley R, Spring-pearson S, Stouthamer R, Nunney L. 2010.
- 709 Multilocus Sequence Typing of *Xylella fastidiosa* Causing Pierce’s disease and Oleander
- 710 Leaf Scorch in the United States. *Ecol Epidemiol* 100:601–611.
- 711 39. Cella E, Angeletti S, Fogolari M, Bazzardi R, De L, Ciccozzi M, Cella E, Angeletti S,
- 712 Fogolari M, Bazzardi R. 2018. Two different *Xylella fastidiosa* strains circulating in Italy:
- 713 phylogenetic and evolutionary analyses. *J Plant Interact* 13:428–432.
- 714 40. Nunney L, Schuenzel EL, Scally M, Bromley RE, Stouthamer R. 2014. Large-scale
- 715 intersubspecific recombination in the plant-pathogenic bacterium *Xylella fastidiosa* is
- 716 associated with the host shift to mulberry. *Appl Environ Microbiol* 80:3025–3033.
- 717 41. Nunney L, Ortiz B, Russell SA, Sánchez RR, Stouthamer R. 2014. The complex
- 718 biogeography of the plant pathogen *Xylella fastidiosa*: Genetic evidence of introductions
- 719 and subspecific introgression in Central America. *PLoS One* 9.
- 720 42. Kabir P, Tumber JMA and KBF. 2014. Pierce’s disease costs California \$104 million per
- 721 year. *Calif Agric* 68:20–29.
- 722 43. Hickey C. 2019. Pierce’s Disease of Grape: Identification and Management. *UGA Coop*
- 723 *Ext Bull* 1514:1–6.
- 724 44. Parker JK, Havird JC, De La Fuente L. 2012. Differentiation of *Xylella fastidiosa* strains
- 725 via multilocus sequence analysis of environmentally mediated genes (MLSA-E). *Appl*
- 726 *Environ Microbiol* 78:1385–1396.
- 727 45. Francis M, Lin H, Rosa JC La, Doddapaneni H, Civerolo EL. 2006. Genome-based PCR
- 728 primers for specific and sensitive detection and quantification of *Xylella fastidiosa*. *Eur J*
- 729 *Plant Pathol* 115:203–213.
- 730 46. Andrews S, Wingett SW, Hamilton RS. 2018. FastQ Screen : A tool for multi-genome
- 731 mapping and quality control [version 2 ; referees : 4 approved] Referee Status :
- 732 F10000research 1–13.
- 733 47. Ewels P, Lundin S, Max K. 2016. Data and text mining MultiQC : summarize analysis
- 734 results for multiple tools and samples in a single report. *Bioinformatics* 32:3047–3048.
- 735 48. Marcel M. 2011. Cutadapt removes adapter sequences from high-throughput sequencing
- 736 reads. *EMB.netJournal* 17:5–7.
- 737 49. Bankevich A. 2012. SPAdes: A New Genome Assembly Algorithm and Its Applications
- 738 to Single-Cell Sequencing. *J Comput Biol* 19:455–477.
- 739 50. Nurk S, Bankevich A, Antipov D, Gurevich A, Korobeynikov A, Lapidus A, Prjibelski A,
- 740 Pyshkin A, Sirotkin A, Sirotkin Y, Stepanauskas R, Clingenpeel S, Woyke T, McLean J,
- 741 Lasken R, Tesler G, Alekseyev M, Pevzner P. 2013. Assembly single-cell genomes and
- 742 mini-metagenomes from chimeric MDA products. *J Comput Biol* 20:714–737.
- 743 51. Rissman AI, Mau B, Biehl BS, Darling AE, Glasner JD, Perna NT. 2009. Reordering

- 744 contigs of draft genomes using the Mauve Aligner. *Bioinformatics* 25:2071–2073.
- 745 52. Seemann T. 2014. Prokka: Rapid prokaryotic genome annotation. *Bioinformatics*
746 30:2068–2069.
- 747 53. Page AJ, Cummins CA, Hunt M, Wong VK, Reuter S, Holden MTG, Fookes M, Falush
748 D, Keane JA, Parkhill J. 2015. Roary : rapid large-scale prokaryote pan genome analysis.
749 *Bioinformatics* 31:3691–3693.
- 750 54. Stamatakis A. 2014. RAxML version 8 : a tool for phylogenetic analysis and post-analysis
751 of large phylogenies. *Bioinformatics* 30:1312–1313.
- 752 55. Paradis E. 2010. Pegas: An R package for population genetics with an integrated-modular
753 approach. *Bioinformatics* 26:419–420.
- 754 56. Mostowy R, Croucher NJ, Andam CP, Corander J, Hanage WP, Martinen P. 2017.
755 Efficient Inference of Recent and Ancestral Recombination within Bacterial Populations.
756 *Mol Biol Evol* 34:1167–1182.
- 757 57. Gu Z, Gu L, Eils R, Schlesner M, Brors B. 2014. circlize implements and enhances
758 circular visualization in R. *Bioinformatics* 30:2811–2812.
- 759 58. Guttman DS, Dykhuizen DE. 1994. Clonal divergence in *Escherichia coli* as a result of
760 recombination, not mutation. *Science* (80-) 266:1380–1383.
- 761 59. Didelot X, Wilson DJ. 2015. ClonalFrameML: Efficient Inference of Recombination in
762 Whole Bacterial Genomes. *PLoS Comput Biol* 11:1–18.
- 763 60. Cohen O, Ashkenazy H, Belinky F, Huchon D, Pupko T. 2010. GLOOME : gain loss
764 mapping engine. *Bioinformatics* 26:2914–2915.
- 765 61. Pfeifer B, Wittelsbu U, Ramos-onsins SE, Lercher MJ. 2014. PopGenome : An Efficient
766 Swiss Army Knife for Population Genomic Analyses in R. *Mol Biol Evol* 31:1929–1936.
- 767 62. Tajima F. 1989. Statistical Method for Testing the Neutral Mutation Hypothesis by DNA
768 Polymorphism. *Genet Soc Am* 595:585–595.
- 769 63. Watterson GA. 1975. On the number of Segregating Sites in Genetical Models without
770 Recombination. *Theor Popul Biol* 276:256–276.
- 771 64. Wright S. 1965. The interpretation of population structure by F-statistics with special
772 regard to systems of mating. *Evolution* (N Y) 19:395–420.
- 773 65. McDonald JH, Kreitman M. 1991. Adaptive protein evolution at the *Adh* locus in
774 *Drosophila*. *Nature* 351:652–654.
- 775 66. Nielsen R, Williamson S, Kim Y, Hubisz MJ, Clark AG, Bustamante C. 2005. Genomic
776 scans for selective sweeps using SNP data. *Genome Res* 15:1566–1575.
- 777 67. Nunney L, Yuan X, Bromley R, Hartung J, Montero-Astúa M, Moreira L, Ortiz B,
778 Stouthamer R. 2010. Population genomic analysis of a bacterial plant pathogen: Novel
779 insight into the origin of Pierce’s disease of grapevine in the U.S. *PLoS One* 5.
- 780 68. Puigbò P, Lobkovsky AE, Kristensen DM, Wolf YI, Koonin E V. 2014. Genomes in
781 turmoil: Quantification of genome dynamics in prokaryote supergenomes. *BMC Med*
782 12:1–19.
- 783 69. Iranzo J, Wolf YI, Koonin E V., Sela I. 2019. Gene gain and loss push prokaryotes beyond
784 the homologous recombination barrier and accelerate genome sequence divergence. *Nat*
785 *Commun* 10.
- 786 70. Hartmann FE, Croll D. 2017. Distinct trajectories of massive recent gene gains and losses
787 in populations of a microbial eukaryotic pathogen. *Mol Biol Evol* 34:2808–2822.
- 788 71. Kettler GC, Martiny AC, Huang K, Zucker J, Coleman ML, Rodrigue S, Chen F, Lapidus
789 A, Ferreira S, Johnson J, Steglich C, Church GM, Richardson P, Chisholm SW. 2007.

- 790 Patterns and implications of gene gain and loss in the evolution of *Prochlorococcus*. PLoS
791 Genet 3:2515–2528.
- 792 72. Moulana A, Anderson RE, Fortunato CS, Huber JA. 2020. Selection Is a Significant
793 Driver of Gene Gain and Loss in the Pangenome of the Bacterial Genus *Sulfurovum* in
794 Geographically Distinct Deep-Sea Hydrothermal Vents. mSystems 5:1–18.
- 795 73. Frick DN, Richardson CC. 2001. DNA Primases. Annu Rev Biochem 70:39–80.
- 796 74. Browning DF, Busby SJW. 2016. Local and global regulation of transcription initiation in
797 bacteria. Nat Rev Microbiol 14:638–650.
- 798 75. Kuo CH, Moran NA, Ochman H. 2009. The consequences of genetic drift for bacterial
799 genome complexity. Genome Res 19:1450–1454.
- 800 76. Albalat R, Cañestro C. 2016. Evolution by gene loss. Nat Rev Genet 17:379–391.
- 801 77. Nunney L, Vickerman DB, Bromley RE, Russell SA, Hartman JR, Morano LD,
802 Stouthamer R. 2013. Recent Evolutionary Radiation and Host Plant Specialization in the
803 *Xylella fastidiosa* Subspecies Native to the United States. Appl Environ Microbiol
804 79:2189–2200.
- 805 78. Kandel PP, Almeida RPP, Cobine PA, De La Fuente L. 2017. Natural Competence Rates
806 Are Variable Among *Xylella fastidiosa* Strains and Homologous Recombination Occurs In
807 Vitro Between Subspecies *fastidiosa* and *multiplex*. Mol Plant-Microbe Interact 30:589–
808 600.
- 809 79. Potnis N, Kandel PP, Merfa M V., Retchless AC, Parker JK, Stenger DC, Almeida RPP,
810 Bergsma-Vlami M, Westenberg M, Cobine PA, De La Fuente L. 2019. Patterns of inter-
811 and intrasubspecific homologous recombination inform eco-evolutionary dynamics of
812 *Xylella fastidiosa*. ISME J 13:2319–2333.
- 813 80. Schmutzer M, Barraclough TG. 2019. The role of recombination, niche-specific gene
814 pools and flexible genomes in the ecological speciation of bacteria. Ecol Evol 9:4544–
815 4556.
- 816 81. Barbosa RL, Rinaldi FC, Guimarães BG, Benedetti CE. 2007. Crystallization and
817 preliminary X-ray analysis of BigR, a transcription repressor from *Xylella fastidiosa*
818 involved in biofilm formation. Acta Crystallogr Sect F Struct Biol Cryst Commun
819 63:596–598.
- 820 82. Barbosa RL, Benedetti CE. 2007. BigR, a transcriptional repressor from plant-associated
821 bacteria, regulates an operon implicated in biofilm growth. J Bacteriol 189:6185–6194.
- 822 83. Guimarães BG, Barbosa RL, Soprano AS, Campos BM, De Souza TA, Tonoli CCC,
823 Leme AFP, Murakami MT, Benedetti CE. 2011. Plant pathogenic bacteria utilize biofilm
824 growth-associated repressor (BigR), a novel winged-helix redox switch, to control
825 hydrogen sulfide detoxification under hypoxia. J Biol Chem 286:26148–26157.
- 826 84. De Lira NPV, Pauletti BA, Marques AC, Perez CA, Caserta R, De Souza AA, Vercesi
827 AE, Paes Leme AF, Benedetti CE. 2018. BigR is a sulfide sensor that regulates a sulfur
828 transferase/dioxygenase required for aerobic respiration of plant bacteria under sulfide
829 stress. Sci Rep 8:1–13.
- 830 85. Federici MT, Marcondes JA, Picchi SC, Stuchi ES, Fadel AL, Laia ML, Lemos MVF,
831 Lemos EGM. 2012. *Xylella fastidiosa*: An *in vivo* system to study possible survival
832 strategies within citrus xylem vessels based on global gene expression analysis. Electron J
833 Biotechnol 15.
- 834 86. Da Silva Neto JF, Koide T, Gomes SL, Marques M V. 2007. The single extracytoplasmic-
835 function sigma factor of *Xylella fastidiosa* is involved in the heat shock response and

- 836 presents an unusual regulatory mechanism. *J Bacteriol* 189:551–560.
- 837 87. Lee KM, Go J, Yoon MY, Park Y, Kim SC, Yong DE, Yoon SS. 2012. Vitamin B 12-
838 Mediated restoration of defective anaerobic growth leads to reduced biofilm formation in
839 *Pseudomonas aeruginosa*. *Infect Immun* 80:1639–1649.
- 840 88. Cordonnier C, Le Bihan G, Emond-Rheault JG, Garrivier A, Harel J, Jubelin G. 2016.
841 Vitamin B12 uptake by the gut commensal bacteria bacteroides thetaiotaomicron limits
842 the production of shiga toxin by enterohemorrhagic *Escherichia coli*. *Toxins (Basel)* 8.
- 843 89. Chen H, De La Fuente L. 2020. Calcium transcriptionally regulates movement,
844 recombination and other functions of *Xylella fastidiosa* under constant flow inside
845 microfluidic chambers. *Microb Biotechnol* 13:548–561.
- 846 90. Cursino L, Li Y, Zaini PA, De La Fuente L, Hoch HC, Burr TJ. 2009. Twitching motility
847 and biofilm formation are associated with tonB1 in *Xylella fastidiosa*. *FEMS Microbiol*
848 *Lett* 299:193–199.
- 849 91. Santos-Beneit F. 2015. The Pho regulon: A huge regulatory network in bacteria. *Front*
850 *Microbiol* 6:1–13.
- 851 92. Singh J, Khan A. 2019. Distinct patterns of natural selection determine sub-population
852 structure in the fire blight pathogen, *Erwinia amylovora*. *Sci Rep* 9:1–13.
- 853 93. Ørsted M, Hoffmann AA, Sverrisdóttir E, Nielsen KL, Kristensen TN. 2019. Genomic
854 variation predicts adaptive evolutionary responses better than population bottleneck
855 history. *PLoS Genet* 15:1–18.
- 856 94. Holderegger R, Kamm U, Gugerli F. 2006. Adaptive vs. neutral genetic diversity:
857 Implications for landscape genetics. *Landsc Ecol* 21:797–807.
- 858 95. Moutinho AF, Bataillon T, Dutheil JY. 2019. Variation of the adaptive substitution rate
859 between species and within genomes. *Evol Ecol*.
- 860 96. Kung SH, Almeida RPP. 2011. Natural competence and recombination in the plant
861 pathogen *Xylella fastidiosa*. *Appl Environ Microbiol* 77:5278–5284.
- 862
- 863
- 864
- 865
- 866
- 867
- 868
- 869
- 870
- 871
- 872
- 873
- 874
- 875
- 876
- 877
- 878

879 **FIGURES LEGENDS**

880 **Figure 1. Maximum Likelihood (ML) tree and haplotype network showing phylogenetic**
881 **and geographic diversification of worldwide PD-causing subsp. *fastidiosa* isolates.** Color
882 represents isolates from the same geographical location: California (Red), Texas (Pink), Georgia
883 (Green), North Carolina (Dark green), Florida (Yellow), Spain (Light blue), and Taiwan (Dark
884 blue). PD-causing strains have been divided into three phylogenetically supported clades (PD-I,
885 PD-II, PD-III). **a.** Haplotype network of PD-causing subsp. *fastidiosa* isolates. Haplotypes
886 belonging to each PD-causing clade are shown within black circles. Roman numbers identify
887 detected haplotypes (I-CXLI). Size of the circle indicates the number of isolates belonging to
888 each haplotype. **b.** Maximum likelihood (ML) tree of PD-causing subsp. *fastidiosa* isolates. Tree
889 was built using the core genome alignment without removing recombinant segments. Bootstrap
890 values mark branch support. Arrows point towards the base of PD-causing clades (-I to -III).

891
892 **Figure 2. Phylogeographic analysis showing diversification of PD-causing isolates within**
893 **the contiguous USA.** Color represents isolates from the same geographical location: California
894 (Red), Texas (Pink), Georgia (Green), North Carolina (Dark green), and Florida (Yellow).
895 Coordinates were recorded during field sampling. In absence of this information, coordinates
896 referred to the city or vineyard closest to the sample site were used. Florida coordinates were not
897 available, the location shown in the map represents central Florida. Isolates from Southern and
898 Northern California are shown within pale red circles. PD-causing strains were divided into three
899 phylogenetically supported clades: PD-I (Southeast USA isolates exclusively), PD-II (Southern
900 California and Texas isolates), and PD-III (both Southern and Northern California isolates, and
901 three Georgia isolates). Tree was built using the core genome alignment without removing
902 recombinant segments. Bootstrap values mark branch support.

903 **Figure 3. Venn diagram and maps showing population linked gene gain/loss events among**
904 **PD-causing isolates.** Color represents isolates from the same geographical location: California
905 (Red), Texas (Pink), Georgia (Green), North Carolina (Dark green), Florida (Yellow), Spain
906 (Light blue), and Taiwan (Dark blue). **a.** Venn diagram shows both the number of genes shared
907 between geographic PD-causing populations and genes unique to each population. Size of the
908 oval represents sample size. **b.** Estimated number of genes gained and lost between geographical
909 locations and following introduction events. Arrows point from the source population to its
910 descendant following introduction events. California isolates belong to the phylogenetically
911 distinct clades PD-II and PD-III. Included Southeast isolates belong to the phylogenetically
912 distinct PD-I and PD-III clades. All maps were publicly available from Wikimedia commons.

913

914 **Figure 4. Frequency and location of recombination events in fastGEAR identified lineages.**

915 Analysis shows results for: **a.** the California/Spain population and **b.** the Southeast USA/Taiwan
916 population. FastGEAR's recombination plots show two distinct lineages on each population (red,
917 PD-III in California/Spain and PD-II/PD-III in Southeast USA/Taiwan; blue, PD-II in
918 California/Spain and PD-I in Southeast USA/Taiwan). The recombination events are shown
919 across the length of the core genome alignment. Larger areas represent recipient sequences while
920 shorter segments of different color within those areas represent donor sequences from another
921 lineage. Recombinant segments from unidentified lineages are shown in black. Maximum
922 Likelihood (ML) trees showing the phylogenetic relationship of isolates within each intra-
923 population cluster identified by fastGEAR are also included. Trees were built using the core
924 genome alignment without removing recombinant segments for the California/Spain and
925 Southeast USA/Taiwan populations. Bootstrap values mark branch support.

926 **Figure 5. Line plot showing variations in Nielsen's composite likelihood ratio (CLR) across**
927 **the length of the core genome alignment (1500 bp window size).** The CLR identifies regions
928 with aberrant allele frequency and determines if their distribution matches those expected from a
929 selective sweep. Peaks represent higher CLR values at that position, which is indicative of a
930 putative selective sweep. Color represents isolates from the same geographical location or
931 phylogenetic cluster. **a.** Lines indicate distinct geographic population: California (Red),
932 Southeast USA (Green), Spain (Light blue), and Taiwan (Dark blue). **b.** Lines indicated distinct
933 phylogenetic clusters: PD-I (Teal), PD-II (Yellow), and PD-III (Purple).

934

935

936

937

938

939

940

941

942

943

944

945

946

947

948

949 **Table 1.** List of genes gained/lost among geographic and phylogenetic PD-causing groups.

| Annotation |
|--|
| Genes absent in the Taiwan population (Found in the contiguous USA) |
| Site-specific DNA-methyltransferase (QIS25725.1); ko:K00571,ko:K00590,ko:K07319 (adenine-specific DNA-methyltransferase); PF01555 |
| Hypothetical protein (QIS26419.1) |
| Peptidoglycan DD-metalloendopeptidase family protein (QIS26766.1); PF06594, PF00353 (RTX calcium-binding nonapeptide repeat) |
| Site-specific DNA-methyltransferase (QIS25737.1); ko:K00571,ko:K00590,ko:K07319 (adenine-specific DNA-methyltransferase); PF01555 |
| Pseudogene |
| Genes absent in the Spanish population (Found in the contiguous USA) |
| CPD*: LacZ, Beta-galactosidase/beta-glucuronidase; ko:K01192(beta-mannosidase) |
| Glutamate 5-kinase (AAO28181.1); ko:K00931; PF00696 |
| PD-II and PD-III exclusive genes in the California population |
| Alpha/beta fold hydrolase (QIS25057.1); ko:K02170,ko:K07002 (pimeloyl-[acyl-carrier protein] methyl ester esterase) |
| Hypothetical protein (QJP55224.1); PF04014 (Antidote-toxin recognition MazE, bacterial antitoxin) |
| Hypothetical protein (AAO28982.1) |
| PD-I and PD-III exclusive genes in the Southeast population, excluding the Taiwanese clade |
| Hypothetical protein (QIS26118.1) |
| Phage head morphogenesis protein (QIS26295.1); PF04233 |
| Genes gained after introduction into Taiwan |
| CPD*: OM_channels Superfamily, Porin superfamily |
| CPD*: DUF769 Superfamily; ko:K15125 (filamentous hemagglutinin) |
| CPD*: entero_EhxA Superfamily |
| Hypothetical protein (QIS25070.1); RTX toxin (QIS25071.1) |
| Genes gained after introduction into Spain |
| Pseudogene: Glycoside hydrolase family 125 protein; ko:K09704 (uncharacterized protein); PF06824 (Metal-independent alpha-mannosidase) |
| DUF596 domain-containing protein (QIS26773.1); PF04591 |
| Hypothetical protein (QID15519.1) |
| Hemagglutinin (QID15518.1); ko:K02014 (iron complex outer membrane receptor protein) |
| 950 ko: KEGG orthology; PF: Pfam database entry ID |
| 951 |
| 952 |
| 953 |
| 954 |

955 **Table 2.** Diversity and neutrality statistics of PD-causing isolates. a) Geographically divided
956 populations, and b) Phylogenetically divided populations.

| Population (a) | Core (nt) | SNPs | π | θ | Tajima's D |
|--------------------|------------|------|------------------------|------------------------|------------|
| California (140) | | 458 | 3.22×10^{-06} | 1.64×10^{-05} | -1.448 |
| Southeast USA (31) | 14,446,213 | 947 | 1.36×10^{-05} | 5.75×10^{-06} | -0.658 |
| Spain (2) | | 2 | 1.38×10^{-07} | 1.38×10^{-07} | * |
| Taiwan (2) | | 6 | 4.15×10^{-07} | 4.15×10^{-07} | * |

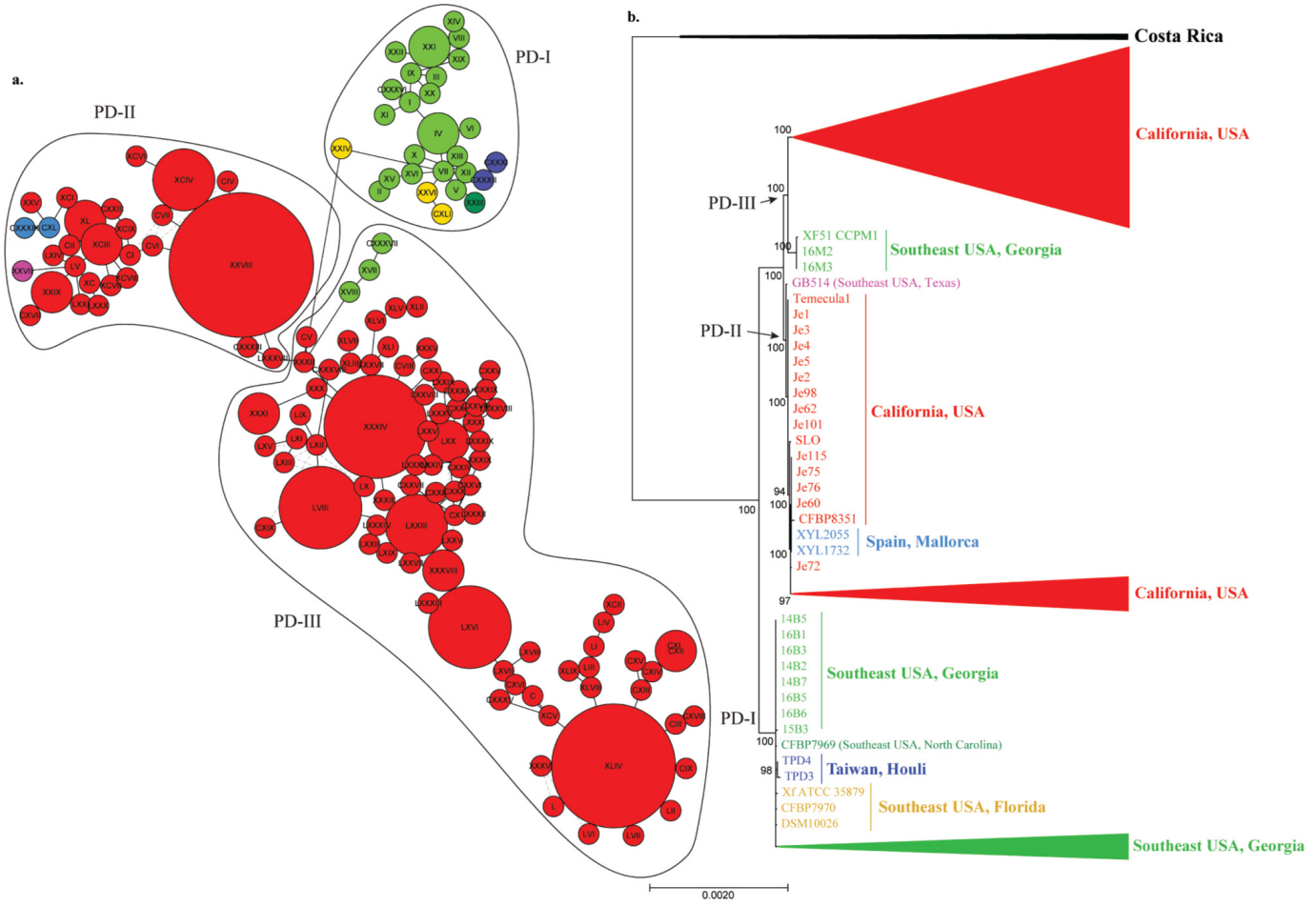
* Spain isolates were not included.

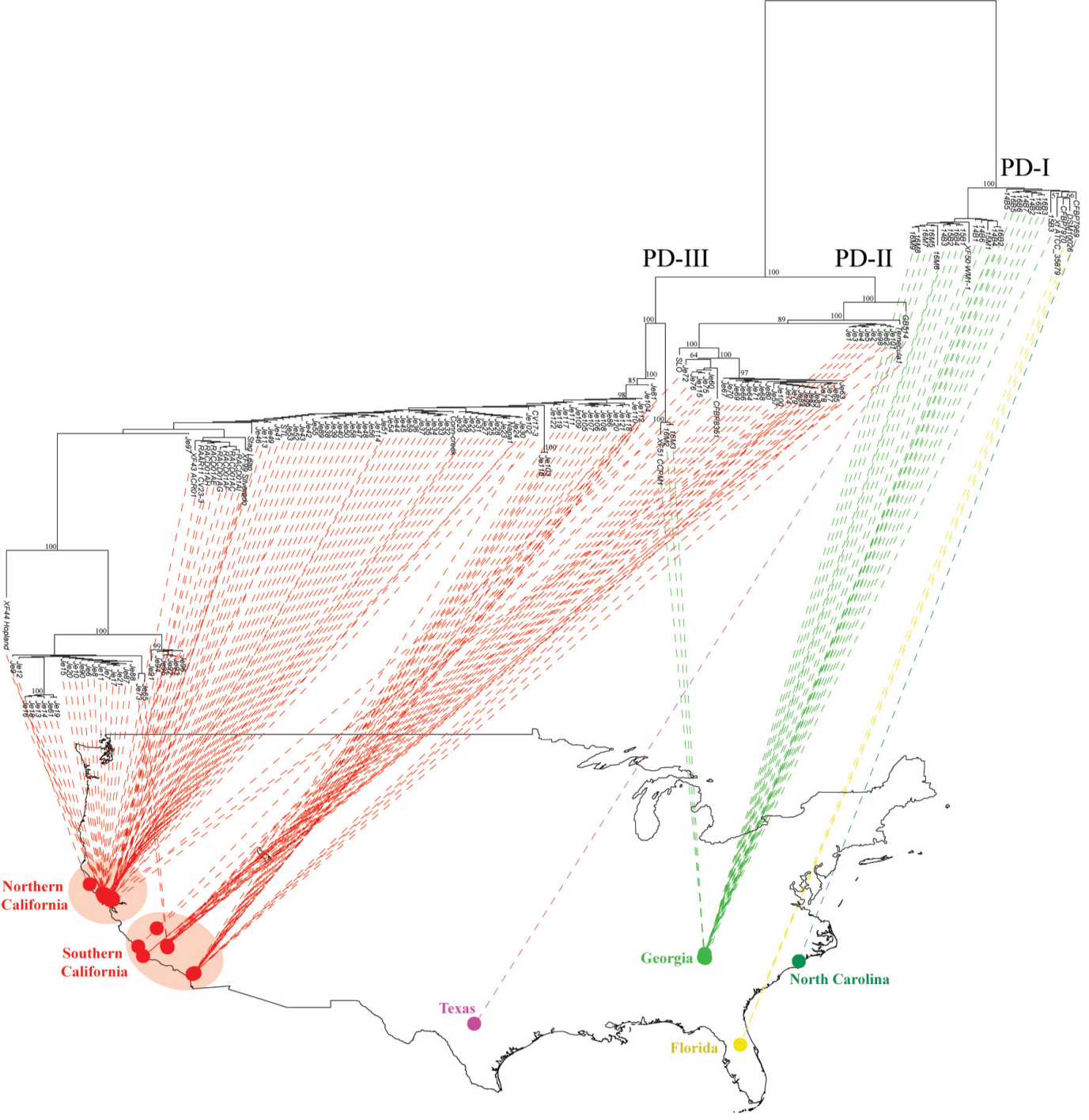
* Taiwan isolates were not included.

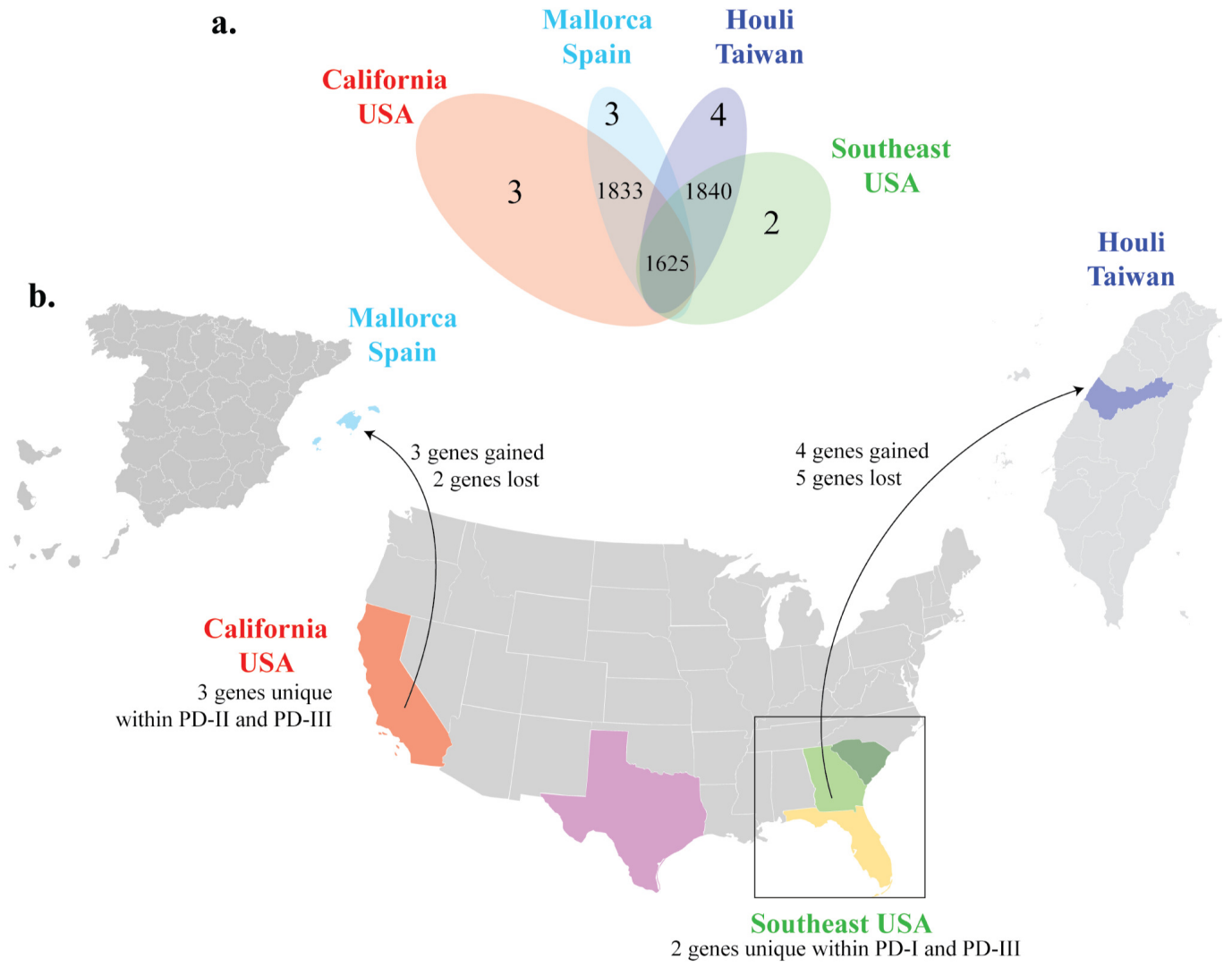
957

| Population (b) | Core (nt) | SNPs | π | θ | Tajima's D |
|----------------|------------|------|------------------------|------------------------|------------|
| PD-I (29) | | 93 | 7.58×10^{-07} | 1.64×10^{-06} | -2.0604 |
| PD-II (40) | 14,446,213 | 114 | 9.65×10^{-07} | 1.87×10^{-06} | -1.7813 |
| PD-III (106) | | 509 | 3.25×10^{-06} | 6.72×10^{-06} | -1.7425 |

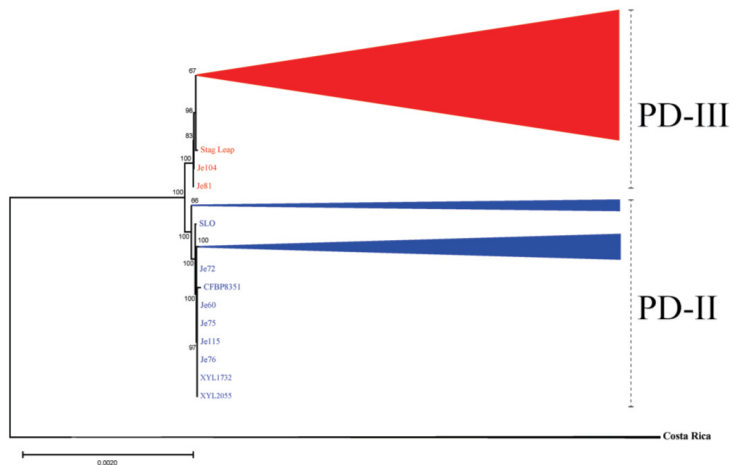
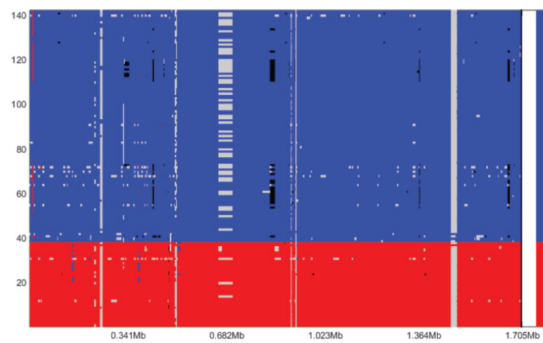
958







a. California/Spain



b. Southeast USA/Taiwan

